Efficient photocatalytic hybrid Ag/TiO_2 nanodot arrays integrated into nanopatterned block copolymer thin films†

Dinakaran Kannaiyan,[a] Min-Ah Cha,[a] Yoon Hee Jang,[a] Byeong-Hyeok Sohn,[b] June Huh,[c] Cheolmin Park[c] and Dong Ha Kim*[a]

Received (in Montpellier, France) 9th June 2009, Accepted 29th June 2009
First published as an Advance Article on the web 10th August 2009
DOI: 10.1039/b9nj00245f

Well defined, ordered arrays of hybrid Ag/TiO_2 hetero nanodots were fabricated on solid substrates using amphiphilic poly(styrene-block-ethylene oxide) diblock copolymer (PS-*b*-PEO) micelles loaded with $AgNO_3$ and TiO_2 sol–gel precursors as templates. The inorganic precursors were selectively incorporated into PEO domains due to specific chemical affinity. The conversion of $AgNO_3$ to metallic Ag was induced by UV irradiation and confirmed by the presence of a surface plasmon band in the UV–vis absorbance spectra. The organic matrix has been removed by deep UV irradiation, leading to arrays of Ag/TiO_2 composite nanoparticles (NPs). The morphology and photocatalytic activities of the resulting hybrid nanoparticle arrays were studied. Markedly enhanced photocatalytic degradation of methylene blue has been observed for Ag/TiO_2 nanodot arrays compared with pure TiO_2 NP arrays.

Introduction

Nanocrystalline titanium oxide (TiO_2) has been extensively studied owing to its outstanding physical and chemical properties in photocatalytic and photovoltaic applications.[1–4] In the context of these applications, the large band gap (3.2 eV) of TiO_2 has been recognised as one of the crucial issues to be resolved since such an inherent property significantly limits the broad applications of the TiO_2 nanostructures under visible light. Thus, the development of a TiO_2 photocatalyst with visible light activity has attracted much attention over the past several years. Typical pioneering efforts to modify TiO_2 include anion doping,[5–8] transition metal ion implantation,[9,10] dye sensitization,[11–14] nitrogen doping,[15] Pt modification[16] and hybridization with noble metals. Among these, composites of noble metal and TiO_2 have been shown to have a high quantum yield of TiO_2 photocatalytic activity by prohibiting the fast recombination of photogenerated charge carrriers.[17] For instance, Ag/TiO_2 and Au/TiO_2 hybrids were reported to have excellent photophysical properties.[18–20] Corno *et al.* reported silver seeded anatase TiO_2 by a diffusion controlled self assembly process.[20b] However, integration of multicomponents with tailored morphology and composition into well defined, ordered arrays is key to ensuring the faithful functioning of the composite nanomaterials. Conventional fabrication methods like photolithography,[21] X-ray lithography,[22] and electron beam lithography[23] have been employed to generate hybrid TiO_2 systems. However, more facile, cost effective means of fabrication along with controlled properties are required for practical applications.

The self assembly of inorganic nanoparticle (NP)/block copolymer (BCP) hybrid systems has been actively studied in recent years due to the abundant types of morphologies and constitutions that can be accessed. For instance, highly ordered 2-D NP arrays with controlled size and interparticle spacing have been suggested using amphiphilic diblock copolymers as templates.[24–27] Typical examples include the fabrication of inorganic nanopatterns derived from polystyrene-*b*-poly(ethylene oxide) diblock copolymer (PS-*b*-PEO) inverse micelles, having insoluble PEO as a core and soluble PS as a corona, with inorganic precursors selectively incorporated into hydrophilic PEO domains.[28] Extending this methodology, hybrid Au/TiO_2 NP arrays were also deduced by incorporating two kinds of inorganic precursors into PS-*b*-PEO templates.[29] However, the spatial distribution of Au NPs in Au/TiO_2 domains was not clarified, nor was any synergistic effect from such a hybrid system reported in our previous work. Although there have been several discussions of similar strategies to fabricate multicomponent NPs embedded in BCP thin films,[30] any particular advantages or enhanced effects from the synergistic combination of the constituent inorganic moieties have not been discussed sufficiently.

Herein, we suggest a facile route to the fabrication of nanodot arrays of hybrid Ag/TiO_2 hetero NPs, using micellar monolayer films of PS-*b*-PEO loaded with TiO_2 sol–gel precursors and $AgNO_3$ salts, as templates. We demonstrate that an improved photocatalytic activity of TiO_2 is achieved by the incorporation of Ag NPs.

[a] *Department of Chemistry and Nano Science, Ewha Womans University, 11-1 Daehyun-Dong, Seodaemun-Gu, Seoul 120-750, Korea. E-mail: dhkim@ewha.ac.kr; Fax: +82-2-3277-4517; Tel: +82-2-3277-3419*
[b] *Department of Chemistry, NANO Systems Institute, Seoul National University, Seoul 151-747, Korea*
[c] *Department of Materials Science and Engineering, Yonsei University, Seoul 120-749, Korea*

† Electronic supplementary information (ESI) available: Phase contrast AFM images of hybrid PS-*b*-PEO/TiO_2/Ag thin films with different constituent compositions. See DOI: 10.1039/b9nj00245f

Experimental section

Materials

Asymmetric poly(styrene-block-ethylene oxide) block copolymer (PS-*b*-PEO) with a polydispersity index of 1.05 was purchased from Polymer Source, Inc. The number average molecular weights (M_n) of PS and PEO blocks are 20 000 g mol^{-1} and 6500 g mol^{-1}, respectively. Titanium tetra-isopropoxide (TTIP, 97%) and $AgNO_3$ were purchased from Aldrich and used as received. Analytical grade toluene, isopropanol and glacial acetic acid were purchased from Laborbedarf GmbH.

TiO_2 sol–gel precursor solution

The sol–gel titania precursor solution was prepared by adding glacial acetic acid (0.342 g) into isopropanol (0.951 g) containing titanium tetraisopropoxide (TTIP) (0.1 g). The mixture was stirred for 6 h, diluted by adding 1 mL of toluene and stirred again for 24 h.

Substrates

Silicon (Si) wafers with a native oxide layer (*ca.* 2.5 cm × 2.5 cm, n-type) were cleaned with 2% Helmanox solution, thoroughly rinsed with Milli-Q water, and then blown dry with nitrogen gas.

Film preparation

0.1 mL of TiO_2 sol–gel precursor was mixed with $AgNO_3$ (molar ratio to EO = 0, 0.02, 0.06, 0.1) by stirring for 10 min and then 0.9 mL of 1 wt% PS-*b*-PEO in toluene was subsequently added. The resulting solution was stirred for 12 h to prepare clear common solution. The amount of precursors relative to the BCPs was varied from 10 to 20.0 v/v%. The hybrid inorganic (TiO_2/Ag)–organic polymer films (Table 1) were produced simply by spin-coating the mixture solution on a piece of silicon substrate at 2000 rpm for 60 s. The obtained films were dried under ambient conditions and exposed to UV light having 254 nm wavelength for 24 h to generate pure TiO_2/Ag nanodot arrays.

Characterization

The morphological studies were carried out with a Digital Instruments 5000AFM (DI/Veeco, Santa Barbara, USA) operated in tapping mode. High resolution transmission electron microscopy (HRTEM) and energy dispersive spectroscopy (EDS) measurements were carried out on a JEOL JSM2100-F at 100 kV. UV–vis absorption studies were carried out using a UV–vis Near IR spectrophotometer (Varian, Cary 5000).

Table 1 Composition of PS-*b*-PEO/TiO_2/Ag thin films

Sample	Polymer (1 wt%) in toluene/mL	TiO_2 sol–gel precursor/mL	$AgNO_3$ (mole ratio to EO)
PS-*b*-PEO/TiO_2	0.9	0.1	
PS-*b*-PEO/TiO_2/Ag_2	0.9	0.1	0.02
PS-*b*-PEO/TiO_2/Ag_6	0.9	0.1	0.06
PS-*b*-PEO/TiO_2/Ag_{10}	0.9	0.1	0.10

Results and discussion

The overall procedure to fabricate arrays of Ag/TiO_2 composite nanodots is schematically illustrated in Scheme 1. TiO_2 sol–gel precursor solution and $AgNO_3$ are mixed with the micellar solution of PS-*b*-PEO in toluene, where the inorganic precursors are selectively incorporated into the PEO domains due to their specific affinity. In practice the TTIP precursor is coupled with the EO units by coordinative interaction after the EO units are protonated by the acidic sol–gel precursor. Spin coating the organic–inorganic solution on silicon substrates produces hybrid thin films. Arrays of pure TiO_2/Ag composite NPs are obtained after removal of the BCP template by UV etching for 24 h. The film thickness was measured to be ~40 nm by AFM sectional analysis.

Upon exposure of the hybrid thin films containing metal precursor to UV light, the colour of the sample turns to brown within 30 min of irradiation, indicating that the $AgNO_3$ precursors were reduced to metallic Ag.[18] This was further confirmed by a UV–vis spectroscopy study. Fig. 1 shows

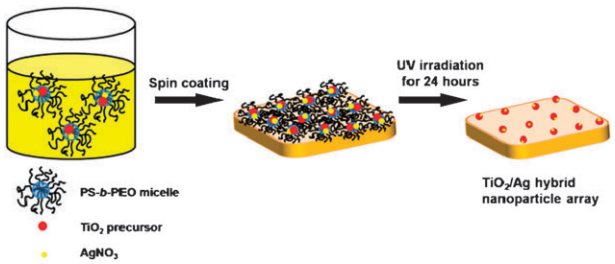

Scheme 1 Schematic diagram of the generation of self-assembled hybrid nanodot arrays of Ag/TiO_2 in PS-*b*-PEO thin films. 1 wt% PS-*b*-PEO in toluene is mixed with TiO_2 sol–gel precursor and $AgNO_3$ salt. The common solution is spin cast on a quartz or a silicon substrate for photocatalytic and morphological studies, respectively. White and red dots in the scheme represent $AgNO_3$ and TiO_2 sol–gel precursor, respectively.

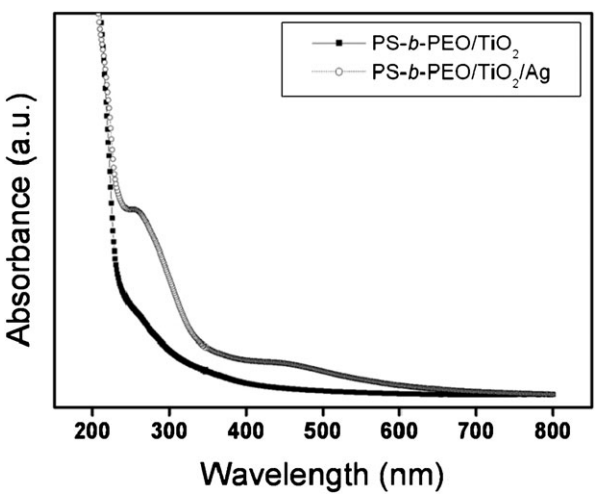

Fig. 1 UV–vis absorbance spectra of PS-*b*-PEO/TiO_2/Ag and PS-*b*-PEO/TiO_2 thin films. The broad absorption at 400–450 nm is attributed to the surface plasmon resonance (SPR) of metallic Ag nanoparticles. The enhanced absorption below 400 nm with the addition of Ag is related to the high refractive index of TiO_2 being in contact with the Ag surface.

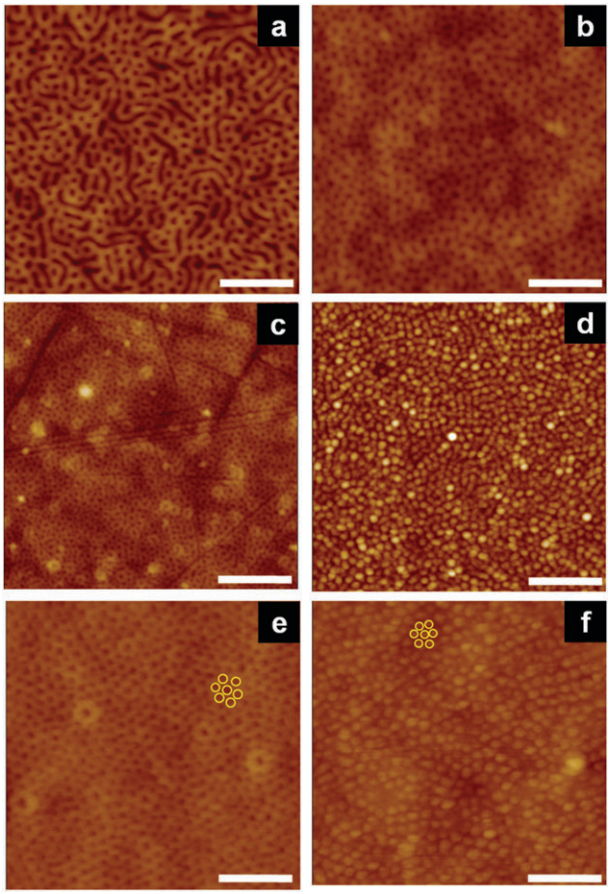

Fig. 2 Height contrast AFM images of PS-*b*-PEO/TiO_2/Ag thin films spin coated on silicon wafers: (a) PS-*b*-PEO/TiO_2, (b) PS-*b*-PEO/TiO_2/Ag2, (c) PS-*b*-PEO/TiO_2/Ag6, (d) PS-*b*-PEO/TiO_2/Ag2 after UV irradiation for 24 h, (e) PS-*b*-PEO/TiO_2/Ag2 solvent annealed and (f) PS-*b*-PEO/TiO_2/Ag2 thermal annealed at 180 °C for 20 h. The scale bar represents 250 nm in length. A fixed amount, 10 vol% of TiO_2 with respect to the BCP, was added to all the samples.

the UV–vis absorption spectra of PS-*b*-PEO/TiO_2 and PS-*b*-PEO/TiO_2/Ag thin films. A broad absorption at 400–450 nm is observed in the UV–vis spectrum of a PS-*b*-PEO/TiO_2/Ag composite film. This band is attributed to the surface plasmon resonance (SPR) of metallic Ag nanoparticles. Comparing the spectrum of the PS-*b*-PEO/TiO_2/Ag film with that of PS-*b*-PEO/TiO_2, it is distinctly observed that the overall absorbance has markedly increased due to the incorporation of Ag NPs. This observation may be of critical impact to photophysical areas of research including the visible light photocatalytic activity or photovoltaic applications of TiO_2. It is also noteworthy that the absorption of TiO_2 below 400 nm was dramatically enhanced with the addition of a small amount of Ag: this spectral feature is related to the high refractive index of TiO_2 in contact with the Ag surface.[31] The increase in the refractive index of TiO_2 significantly alters scattering, which results in a strong increase in the absorbance at shorter wavelengths.

The morphologies of the PS-*b*-PEO block copolymer thin films with TiO_2 sol–gel precursor and $AgNO_3$ were studied by AFM. Fig. 2 shows a series of height contrast AFM images of PS-*b*-PEO with TiO_2 sol–gel precursor and $AgNO_3$ in different amounts, before and after UV treatment. The molar ratio of $AgNO_3$ was varied, with the amount of sol–gel precursor solution being fixed at 10 vol%. The AFM image of an as cast PS-*b*-PEO/TiO_2 film in Fig. 2(a) shows mixed wire and quasi-hexagonal nanodot arrays. Upon the addition of Ag, the ternary hybrid film exhibits quasi-hexagonal arrays with improved order, with a relatively uniform domain size as shown in Fig. 2(b) and 2(c). In order to induce arrays of improved quasi-hexagonal packing arrangement, the as cast films were subjected to solvent vapours and thermal annealing (Fig. 2(e) and 2(f)), where local hexagonal assembly of domains is clearly observed (marked with yellow circles). The morphology of a micelle depends on three basic factors:[32] (1) the stretching of the core-forming chains, (2) the core–corona interfacial energy, and (3) the repulsion among coronal chains. These factors are associated with Gibbs free energy of the micelles, if it were the enthalpic or entropic term. A change in any one of these parameters would lead to a change of the morphology in order to reach a new stable state. When TiO_2 sol–gel precursor solution and $AgNO_3$ are mixed with a micellar solution of PS-*b*-PEO in toluene, the inorganic precursors are selectively incorporated into the PEO domains. The EO units are protonated by the acidic sol–gel precursor to become polar and then blended with inorganic precursor. In our system, addition of $AgNO_3$ leads to well ordered quasi-hexagonal arrays of micelles. However, incorporation of a larger amount of $AgNO_3$ results in a less ordered morphology because the PEO/titania domains cannot accommodate the precursors over a certain boundary. The effect of additives on the morphologies of hybrid titania films has been discussed in detail in our previous reports.[28,33] Such an optimum NP and sol–gel content in terms of the improved order observed for the hybrid films was independent of the film thickness in the range of 10–50 nm used in this study. A further increase in the amount of $AgNO_3$ in the PS-*b*-PEO/TiO_2 hybrid results in disordered and complicated morphologies (Fig. 2c, supporting information Fig. S1 and S2†). Such effects of NP inclusion on the generation of more complicated morphologies have been reported by Balazs *et al.*[34] Fig. 2d shows the AFM topology of a PS-*b*-PEO/TiO_2/Ag film after a UV irradiation

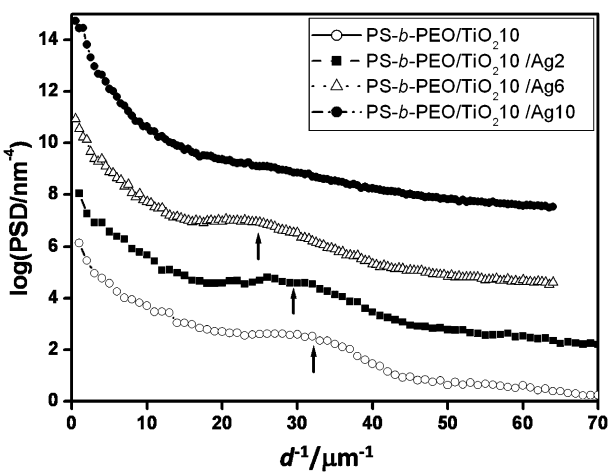

Fig. 3 Power spectral density profiles calculated from the AFM images in Fig. 2.

of 24 h. UV etching completely removes BCP from the hybrid film, leaving pure NP arrays on the substrate. A corresponding series of phase contrast AFM images was also studied for the same films, following morphological variation as well as the change of modulus contrast upon the addition of TiO_2 and Ag into PS-*b*-PEO (see Fig. S1 in the supporting information†). The average centre-to-centre distance (d_{C-C}) of neighbouring particles was evaluated by the peak position of the power spectral density (PSD) profiles converted from AFM images as shown in Fig. 3. The d_{C-C} values obtained from PSD patterns are measured to be ~33, 31, and 24 nm for samples of fixed TiO_2 sol–gel amount of 10 vol%, with Ag 0, 2, and 6, respectively. The PSD peak in the sample containing TiO_2 sol–gel 10 vol% and Ag10 is significantly broadened, indicating a decrease of structural control (see Fig. S2 of supporting information†). TEM experiments were carried out to evaluate the diameter as well as to further probe the internal structure of the hybrid nanodot. To this end, a hybrid film was prepared by drop casting a PS-*b*-PEO/TiO_2/Ag2 solution on a carbon coated copper grid. Fig. 4 shows a representative TEM and EDS spectrum obtained from a composite film. The diameter of the nanodomains in PS-*b*-PEO/TiO_2/Ag2 film is measured to be ~35 to 40 nm. It is observed that the micellar core domains with inorganic moieties are arranged in a quasi-hexagonal packing (indicated by yellow circles in Fig. 4(a)). A magnified view of an individual NP obtained by HRTEM reveals a typical crystalline Ag lattice structure, which is in contact with TiO_2 domains (Fig. 4(b)). The obtained TiO_2 is found to be crystalline, as evidenced by the lattice structure in the background of the Ag lattice. It has been reported that crystalline TiO_2 would show higher photo-activity than an amorphous one.[35] The chemical identity of the hybrid film was also confirmed by EDS data, where the presence of Ag and TiO_2 is evident (Fig. 4(c)).

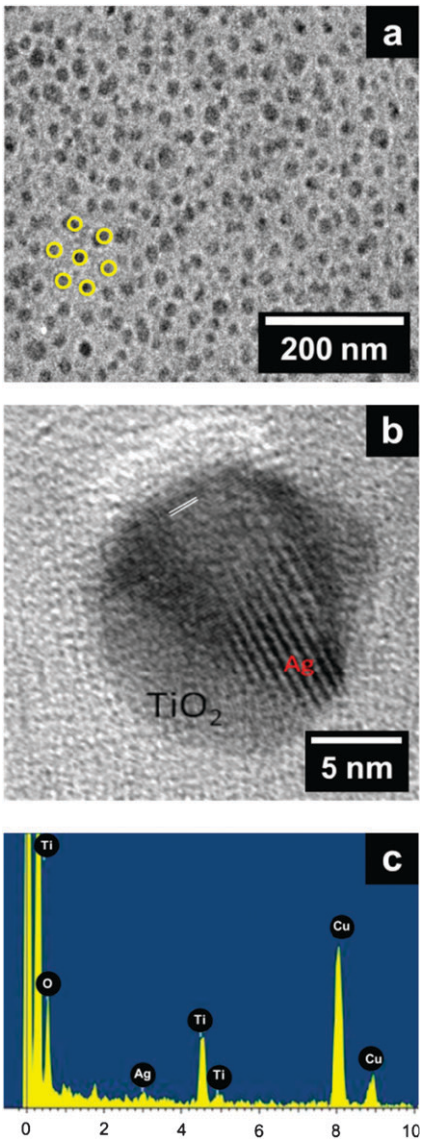

Fig. 4 TEM image (a), HRTEM image (b), and EDS spectra (c) of PS-*b*-PEO/TiO_2/Ag2 film. TEM samples were prepared by drop casting a PS-*b*-PEO/TiO_2/Ag mixture solution on a carbon coated copper grid followed by exposure to UV light for 2 h.

In order to explore any synergistic properties that such hybrid TiO_2/Ag hetero nanostructures may possess, the photocatalytic efficiency of the PS-*b*-PEO/TiO_2/Ag system was compared with PS-*b*-PEO/TiO_2 to assess the degradation of methylene blue (MB) under UV–vis light, the results of which are displayed in Fig. 5. The samples on quartz glass

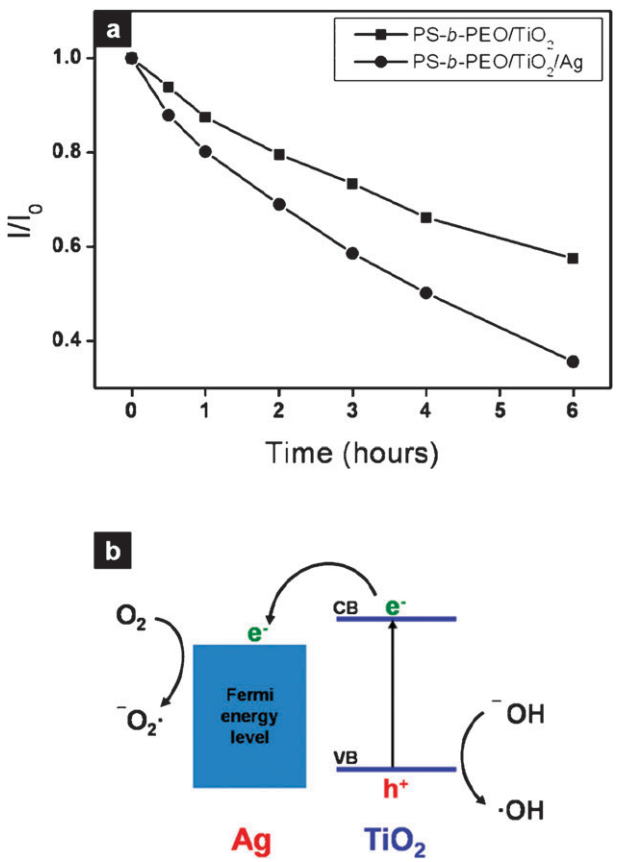

Fig. 5 Photocatalytic degradation of methylene blue (MB): (a) plot of the ratio of the intensity of the peak at 664 nm (I/I_0) with time; (b) energy level diagram of Ag/TiO_2 hetero nanostructures with proposed photocatalytic mechanism. The degradation of MB on a PS-*b*-PEO/TiO_2 thin film was enhanced with ~30% efficiency by the incorporation of Ag.

substrates were immersed in a UV cuvette filled with 10 ppm aqueous MB solution and irradiated with UV light of 254 nm wavelength for a specified length of time. The ratio of the intensity of the absorbance peak at 664 nm, before and after irradiation (I/I_0) was correlated and displayed with time in Fig. 5a. It is found that the degradation of MB on a BCP/TiO_2 thin film was significantly enhanced by the incorporation of Ag NPs, *e.g.*, about a 30% enhancement of the photocatalytic activity was calculated for 0.02 molar ratios of Ag to EO.

The PS-*b*-PEO/TiO_2/Ag thin films almost completely decomposed the MB solution within 7 h, which took more than 10 h for the PS-*b*-PEO/TiO_2 film. A possible mechanism for the enhanced photocatalytic activity can be understood through the energy band diagram in Fig. 5b. The inhibition of the recombination between photoinduced electron–hole pairs, as a result of the migration of the photogenerated electrons from the surface of TiO_2 to the Ag/TiO_2 hetero structure, is believed to be responsible for the enhanced photocatalytic activity of PS-*b*-PEO/TiO_2/Ag.[17b,36,37] Since there is a very low concentration of holes to recombine with, the electrons have a higher probability to participate in the reduction reaction to form active species like super-oxide anion radicals,[38] a very strong oxidant, which can decompose organic substances effectively. The hybrid nanodots were shown to have higher photodegradation capabilities than neat TiO_2 ones, even for a limited surface area. We expect that integration of this type of hybrid into 3D film would lead to much enhanced activity. The protocol and experimental observations discussed in this article may allow for widespread tailored design of similar hetero nanostructures with versatile functions.

Conclusions

We have suggested a simple method to fabricate Ag/TiO_2 composite NP arrays using amphiphilic PS-*b*-PEO diblock copolymer inverse micelles as templates. The selective dispersion of two kinds of NPs in one of the blocks was achieved through polar interactions between the PEO block and the precursors. The addition of Ag into PS-*b*-PEO/TiO_2 films changed the morphology from a mixed wire/hexagonal packing to a well ordered quasi-hexagonal packing arrangement. UV–vis study showed an enhanced absorption for PS-*b*-PEO/TiO_2/Ag films compared with PS-*b*-PEO/TiO_2 films, implying a promising candidate for a visible light active photocatalytic system. The enhanced photocatalytic degradation of MB has been observed in PS-*b*-PEO/TiO_2/Ag thin films due to the inhibition of photoinduced electron–hole recombination as a result of an effective charge transfer between the two inorganic nanodomains.

Acknowledgements

D. Kannaiyan is grateful for the support of a Brain Pool fellowship by KOSFT (081S-2-3-0173). This work was supported by a Korea Science and Engineering Foundation (KOSEF) grant funded by the Korean government (MEST) (No. R11-2005-008-00000-0; R01-2008-000-11712-0).

References

1 (*a*) J. L. Gole, J. D. Stout, C. Burda, Y. Lou and X. Chen, *J. Phys. Chem. B*, 2004, **108**, 1230; (*b*) C. Burda, Y. Lou, X. Chen, A. C. S. Samia, J. Stout and J. L. Gole, *Nano Lett.*, 2003, **3**, 1049.
2 A. Mills, G. Hill, S. Bhopal, I. P. Parkin and S. A. O'Neil, *J. Photochem. Photobiol., A*, 2003, **160**, 185.
3 G. E. Brown, V. E. Henrich, W. H. Casey, D. L. Clark, C. Eggleston, A. Femly, D. W. Goodman, M. Gratzel, G. Macial, M. I. McGarthy, K. H. Nealson, D. A. Sverjensky, M. F. Toney and J. M. Zachara, *Chem. Rev.*, 1999, **99**, 77.
4 B. S. Bilmes, P. Mandelbaum, F. Alvarez and N. M. Victoria, *J. Phys. Chem.*, 2000, **104**, 9851.
5 R. Asahi, T. Morikawa, T. Ohwaki, K. Aoki and Y. Taga, *Science*, 2001, **293**, 269.
6 Y. Sakatani, K. Okusako, H. Koike and H. Ando, *Photocatalysis*, 2002, **4**, 51.
7 H. Irie, Y. Watanabe and K. Hashimoto, *J. Phys. Chem. B*, 2003, **107**, 5483.
8 K. Kobayakawa, Y. Murakami and Y. Sato, *J. Photochem. Photobiol., A*, 2005, **170**, 177.
9 W. Choi, A. Termin and M. R. Hoffmann, *J. Phys. Chem.*, 1994, **98**, 13669.
10 M. Anpo, *Catal. Surv. Jpn.*, 1997, **1**, 169.
11 J. Hodak, C. Quinteros, M. I. Litter and E. San Roman, *J. Chem. Soc., Faraday Trans.*, 1996, **92**, 5081.
12 Y. Cho, C. H. Lee, T. Hyeon and H. I. Lee, *Environ. Sci. Technol.*, 2001, **35**, 966.
13 D. Chatterjee and A. Mahata, *Appl. Catal., B*, 2001, **107**, 119.
14 E. Bae, W. Choi, J. Park, H. S. Shin, S. B. Kim and J. S. Lee, *J. Phys. Chem. B*, 2004, **108**, 14093.
15 (*a*) H. Fu, L. Zhang, S. Zhang, Y. Zhu and J. Zhao, *J. Phys. Chem. B*, 2006, **110**, 3061; (*b*) R. Nakamura, T. Tanaka and Y. Nakato, *J. Phys. Chem. B*, 2004, **108**, 10617; (*c*) G.-R. Torres, T. Lindgren, J. Lu, C.-G. Granqvist and S.-E. Lindquist, *J. Phys. Chem. B*, 2004, **108**, 5995.
16 K.-W. Park, *Inorg. Chem.*, 2005, **44**, 3190.
17 (*a*) M. R. Hoffmann, S. T. Martin, W. Choi and D. W. Bahnemann, *Chem. Rev.*, 1995, **95**, 69; (*b*) J. Sá, M. Fernández-García and J. A. Anderson, *Catal. Commun.*, 2008, **9**, 1991.
18 X. Wang, J. C. Yu, C. Ho and A. C. Mak, *Chem. Commun.*, 2005, 2262.
19 J. Li and H. C. Zeng, *Chem. Mater.*, 2006, **18**, 4270.
20 (*a*) X. Wang, D. R. G. Mitchell, K. Prince, A. J. Atanacio and R. A. Caruso, *Chem. Mater.*, 2008, **20**, 3917; (*b*) J. A. Corno, J. Stout, R. Yang and J. L. Gole, *J. Phys. Chem. C*, 2008, **112**, 5439.
21 G. M. Wallraff and W. D. Hinsberg, *Chem. Rev.*, 1999, **99**, 1801.
22 M. F. Bertino, R. R. Gadipalli, L. A. Martin, L. E. Rich, A. Yamilov, B. R. Heckman, L. Leventis, S. Guha, J. Katsoudas, R. Divan and D. C. Mancini, *Nanotechnology*, 2007, **18**, 315603.
23 T. Ito and S. Okazaki, *Nature*, 2000, **406**, 1027.
24 Y. H. La, M. P. Stoykovich, S. M. Park and P. F. Nealey, *Chem. Mater.*, 2007, **19**, 4538.
25 K. Aissou, T. Baron, M. Kogelschatz, M. Den Hertog, J. L. Rouvière, J. M. Hartmann and B. Pélissier, *Chem. Mater.*, 2008, **20**, 6183.
26 J. Bansmann, S. Kielbassa, H. Hoster, F. Weigl, H. G. Boyen, U. Wiedwald, P. Ziemann and R. J. Behm, *Langmuir*, 2007, **23**, 10150.
27 S. P. Anthony and J. K. Kim, *Chem. Commun.*, 2008, 1193.
28 D. H. Kim, Z. Sun, T. P. Russell, W. Knoll and J. S. Gutmann, *Adv. Funct. Mater.*, 2005, **15**, 1160.
29 (*a*) X. Li, J. Fu, M. Steinhart, D. H. Kim and W. Knoll, *Bull. Korean Chem. Soc.*, 2007, **28**, 1015; (*b*) X. Li, P. Goring, E. Pipell, M. Steinhart, D. H. Kim and W. Knoll, *Macromol. Rapid Commun.*, 2005, **26**, 1173.
30 (*a*) B. H. Sohn, J. M. Choi, S. I. Yoo, S. H. Yun, W. C. Zin, J. C. Jung, M. Kanehara, T. Hirata and T. Teranishi, *J. Am. Chem. Soc.*, 2003, **125**, 6368; (*b*) J. S. Lee, Y. M. Kim, J. H. Kwon, H. Shin, B. H. Sohn and J. Lee, *Adv. Mater.*, 2008, **20**, 1.
31 L. M. Liz-Marza′n, M. Giersig and P. Mulvaney, *Langmuir*, 1996, **12**, 4329.

32 L. Zhang and A. Eisenberg, *J. Am. Chem. Soc*., 1996, **118**, 3168.
33 X. Li, H. Yang, C. Li, L. Xu, Z. Zhang and D. H. Kim, *Polymer*, 2008, **49**, 1376.
34 (*a*) J. Huh, V. V. Ginzburg and A. C. Balazs, *Macromolecules*, 2000, **33**, 8085; (*b*) R. B. Thomson, V. V. Ginzburg, M. W. Matsen and A. C. Balazs, *Science*, 2001, **292**, 2469; (*c*) J. Y. Lee, R. B. Thomson, D. Jasnow and A. C. Balazs, *Macromolecules*, 2002, **35**, 4855.
35 W. Macyk and H. Kisch, *Chem.–Eur. J*., 2001, **7**, 1862.
36 Y. Zheng, L. Zheng, Y. Zhan, X. Lin, Q. Zheng and K. Wei, *Inorg. Chem*., 2007, **46**, 6980.
37 (*a*) P. K. Sudeep, K. Takechi and P. V. Kamat, *J. Phys. Chem. C*, 2007, **111**, 488; (*b*) T. Hirakawa and P. V. Kamat, *Langmuir*, 2004, **20**, 5645; (*c*) T. Hirakawa and P. V. Kamat, *J. Am. Chem. Soc*., 2005, **127**, 3928.
38 (*a*) J. Ryu and W. Choi, *Environ. Sci. Technol*., 2004, **38**, 2928; (*b*) J. R. Nakamura, T. Tanaka and Y. Nakato, *J. Phys. Chem. B*, 2005, **109**, 8920.

